Characterization of Asymmetry in Low-Power Wireless Links: An Empirical Study

Prasant Misra   Nadeem Ahmed   Sanjay Jha

University of New South Wales, Australia
{pkmisra,nahmed,sanjay}@cse.unsw.edu.au

Technical Report
UNSW-CSE-TR-1016
June 2010

THE UNIVERSITY OF
NEW SOUTH WALES

School of Computer Science and Engineering
The University of New South Wales
Sydney 2052, Australia

Abstract

Experimental studies in wireless sensor network (WSN) have shown that asymmetry in low-power wireless links has a significant effect on the performance of WSN network protocols. Protocols, which work in simulation studies often fail when link asymmetry is encountered in real deployments. Characterization of link asymmetry, is thus, of importance for the design and operation of resilient WSN protocols in real scenarios. This paper details an empirical study to characterize link asymmetry in WSNs. It presents a systematic approach to measure the effects of hardware performance, environmental factors, and temporal properties, on link asymmetry, using off-the-shelf WSN devices. It shows that differences in reception power of WSN devices, operating within the receiver's critical sensitivity band of $\approx$ [-80dBm, -90dBm], transmit-receive switching operation, environmental factors, and high traffic load, are the major factors responsible for asymmetry in low-power wireless links, while frequency misalignment in the transmitter, and power variations in the antenna are unlikely causes for it.

1 Introduction

The practical realization of wireless systems are challenged by the assumptions made in the theoretical models, as the wireless medium (i.e. air) is a complex entity to understand, as opposed to the wired medium of communication. The bottleneck in the successful study of wireless systems are not the sophisticated communication devices, but the study of the communication medium with respect to a signal type. Depending on the operating environment, the robustness of such systems are affected by communication channel conditions that may be inhomogeneous and noisy. Therefore, these studies help to analyze the characteristics of the wireless channel with the varying channel conditions, and provide accurate modeling.

The models used in the simulation study of low-powered wireless systems make simplifying assumptions about the characteristics of the wireless link. The properties of these links, as observed in real-world scenarios, differ immensely from these models, especially in their asymmetric nature. Link asymmetry is a common phenomenon observed in such devices utilized in sensor networks, and has significant impact on the performance of various protocols. Protocols, which work in simulation studies often fail, when link asymmetry is encountered in real deployments. Hence, its understanding is vital for designing and developing, reliable and robust, energy efficient protocols with higher throughput that would prolong the network lifetime.

This paper provides an empirical study to characterize link asymmetry in WSNs. It addresses this problem by analyzing the system components (i.e. transmitter, antenna, receiver, switching between transmit-receive modes) and identifying deviations in their functionality, influence of environmental conditions, and long-term temporal properties of the wireless links. We take a different approach to analyze these parameters. In addition to using traditional methods of data collection, and off-line processing and analysis, we capture real-time data by using the spectrum analyzer for many of our experiments. We, not only, establish the correctness of previous work, but also provide new evidence and details in our study. We show that frequency misalignment in the transmit mode, and the standard antennae used in the WSN motes are unlikely causes of link asymmetry. The major factors contributing towards it are difference in reception power of the motes within the receiver's critical sensitivity band of $\approx$ [-80dBm, -90dBm], switching mode of operation, environmental factors, and high traffic load (defined by a low inter-packet interval time).

The remainder of the paper is arranged as follows: Section 2 provides details of our experimental methodology in terms of the radio, hardware and experimental setup (topology) used in our study. Section 3 presents an extensive evaluation of the various factors responsible for the asymmetry problem in links. A review of related work for studies on low-powered wireless links has been discussed in Section 4. Finally, a discussion of future work and conclusion is provided in Section 5.

2 Experimental Methodology

This section describes the low-powered radios, hardware platforms, and our testbed (or topology) utilized in our study.

Chipcon CC1000 [1] and CC2420 [2] radios were used in our evaluation, however, the majority of the experiments were performed using CC2420. CC1000 are 868
/916MHz radios that were used in early sensor network platforms. They support frequency shift keying (FSK) modulation scheme with manchester encoding, and are capable of supporting a maximum data-rate of 38.4KBaud. CC2420 is a ZigBee-complaint 2.4GHz IEEE 802.15.4 radio that can be tuned to scan channels from 11 (2.405GHz) to 26 (2.480GHz), each separated by 5MHz. It uses orthogonal quadrature phase shift keying (OQPSK) and direct sequence spread spectrum (DSSS) to send chips at 2MHz. A data-rate of 250Kbps is achieved by encoding a 4-bit symbol with 32 chips. It measures the RF signal strength of the received packet (in dBm) by averaging over eight symbol periods (128μs.).

The experiments were performed using Mica2 [3] and MicaZ [4] motes as the primary hardware platforms. A detachable monopole antenna of one-quarter wavelength insulated wire is attached to these motes through the MMCX connector. The length of the antenna is 3.20inches and 1.20inches respectively, for each of these platforms.

Different experimental setups were created for the evaluation.

Setup-A: A pair of sensor motes powered by AA batteries (1.5V-1.6V) were utilized, wherein the sender mote transmits 6000 broadcast packets, each of length 29 Bytes, at the rate of 100 packets/second to the base station (receiver mote) with an inter-packet interval (IPI) of 10msec., and highest transmission power of 0dBm. The base station (BS) logs the received signal strength indicator (RSSI), link quality index (LQI), and sequence number (SN) of every packet to a laptop over the wired medium.

Setup-B: It is the wired version of Setup-A. The antennae were removed from the respective motes. They were connected to a spectrum analyzer (SA) by a coaxial cable through an attenuator (configured with an attenuation level of 25dBm).

Setup-C: A straight-line topology was created by using 4 MicaZ motes (numbered 0,3,5,7). Mote 0 was configured as the BS, and the remaining motes 3, 5, 7 were placed at a distance of 1m, 5m, 10m from mote 0. Mote 3, 5, 7 send data packets containing the SN in the payload to mote 0, which receives and sends an acknowledgment packet to the respective sender, by copying the SN of the received packet into the payload. The RF transmit power was set at its minimum level of -25dBm to create intermediate links as described in Section 3.6.

All the motes are connected to a logging workstation that records the RSSI, LQI and SN of each packet exchanged. They were interfaced with programming boards, powered by the line current, thereby eliminating any irregularities in observed data due to variation in supply power levels, that may crop up with the exhaustion of the battery power. This setup was used with different configuration of IPI of 100msec, 200msec and 1000msec, and packet length (PL) of 29Bytes, 39Bytes and 49Bytes, each for a period of 24 hours.

Setup-D: This is the non-switching version of Setup-C, wherein the BS (only) broadcasted packets to the motes 3,5,7, while all other parameters and configurations remained the same.

3 Performance Evaluation

3.1 Transmitter

The aim of this study was to capture the effect of using different radio transceivers (in the transmit mode) on frequency misalignment. The observation data was collected using experimental Setup-A in an indoor office environment. Anritsu's spectrum analyzer (SA), bearing model number MS2721A [5], was used to capture the spectrum envelope of the transmitting mote. The SA was configured to the maximum-hold level, so as to lock the maximum power level of the transmitted packets in every frequency sweep. This exercise was cyclically repeated for 4 different motes of each type (Mica2 and MicaZ). The motes and the SA were tuned to their nominal center frequencies, which is 2.480GHz for MicaZ (channel 26) and 916.7MHz for Mica2 motes.

Figures 3.1-(a) and (b) show the peak envelope levels, observed at each frequency slot, during the process of data transmission for Mica2 and MicaZ motes, respectively. The Mica2 and MicaZ motes show a peak envelope variation between [-30dBm,-36dBm] and [-43dBm,-50dBm] respectively. In addition, the motes were observed to transmit at their designated center frequency within their specified bands.

These results show that all the motes do transmit in the frequency band allocated for the specified channel, and that the spectrum occupied by each motes transmission are similar with no significant frequency offsets. In addition, power variations were also observed in the (measured) received power for the different motes, which varied within 6-7dBm for both Mica2 and MicaZ motes. The reason for this variation can be accounted to the manufacturing process, where the fabricated motes are similar but not the same in their built, and therefore there are small discrepancies in the power level of the transmitted packets, which are close to the specified power level, but, do not match exactly. It is interesting to note that, even when we transmit packets at 0dBm, there is a substantial decrease in RF power before the packets are sniffed by the SA (which is placed very close to the transmitting motes).

We conclude that the wireless medium is lossy, even in short distances (specific to the experimental environment), and also that, frequency misalignment in the transmit mode cannot be accounted for link asymmetry. Thus, our results differ from Liu et. al. in [6], where it has been reported that different motes show large differences in transmission power [0dBm,-14dBm], and their respective spectra are shifted to the extent that they overlap partially.

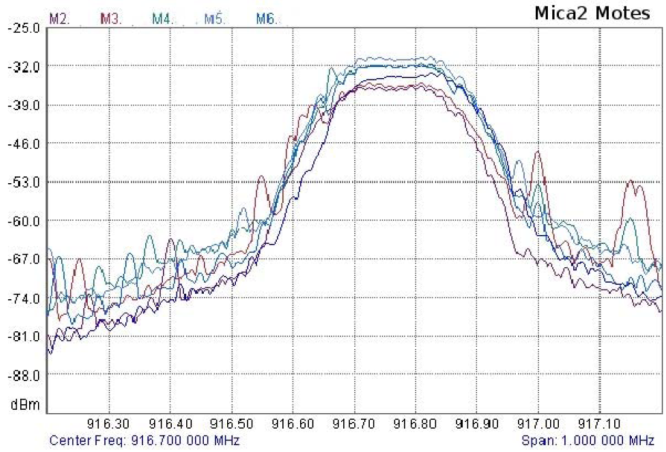

(a): Mica2.

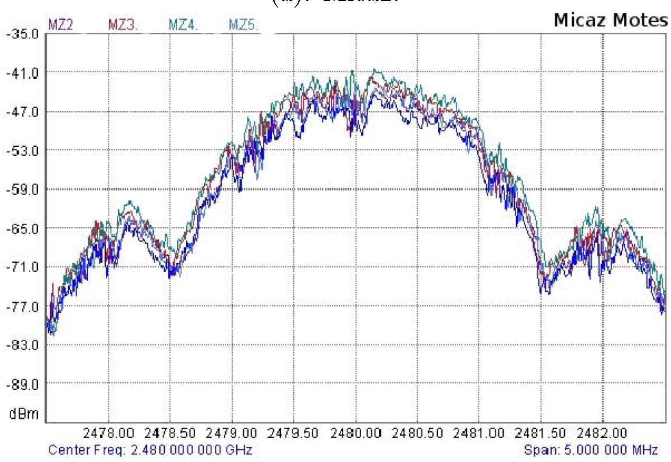

(b): MicaZ.

Figure 3.1: Spectrum envelope of Tx mote(s).

3.2 Antenna

The study, in this section, was conducted to analyze the effect on spectral variations, with the use of the wired medium instead of the wireless antennae, and compare it with the wireless transmission experiments. It was performed using Setup-B in an indoor office environment using four different Mica2 motes. The SA settings were configured as described in the Section 3.1.

Figure 3.2 shows the result obtained from this wired setup. The Mica2 motes show a peak envelope variation between [-27dBm,-34dBm], thereby displaying a variation of $\approx$ 7dBm. We also observe a few peaks surrounding the center frequency band, which may be due to the presence of other radio devices operating in the place of experimentation.

A comparison of the result with Figure 3.1-(a) shows near identical spectrum results for the wired and wireless setups of the same experiment. The only noticeable difference is that the peak power level has changed from -30dBm (pre-

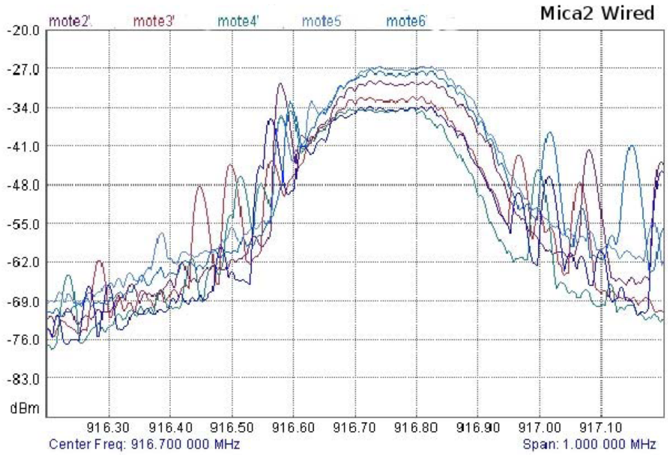

Figure 3.2: Spectrum envelope of Tx mote(s). Mica2: Wired.

vious) to -27dBm(current), which is due to the change in the transmit power from 0dBm to -25dBm (due to the attenuator). We, also, observe that the power level of the transmitting packets set through the attenuator (at -25dBm), gets depreciated ($\approx$ 2dBm)in its propagation over the short physical wired medium.

This indicates that the standard (*untampered*) antennae used in the motes does not have a significant effect on the received power, and hence is not a major contributor to link asymmetry.

3.3 Receiver

In this section, we characterize the receiver, using a set of MicaZ motes. We found that the motes transmitting a 0dBm power were able to successfully send and receive packets, without the need of any antennas or wires, when placed at a distance of about 1m from each other. This is due to the energy leakage, which was circumvented by placing an attenuator between the transmitter and receiver motes, as mentioned in Setup-B. The attenuation values were varied to control the packet reception rate (PRR) corresponding to the condition of minimum to maximum attenuation or received signal strength (RSS) at the receiver.

Figure 3.3 compares the PRR against RSS for different receiver motes. The results show that the PRR drops from 100% to 0% over a range of about 8dBm in attenuation, or decrease in RSS, and in addition, different motes show different response characteristics to the change in received power levels. All motes show a 100% PRR at attenuation values $<$ 54dBm, while none of them are able to receive any packets with attenuation $>$ 62dBm.

The actual RSS values at the motes can be obtained by considering the mote's transmission power(-25dBm), power loss over the wired medium($\approx$ 2dBm), and the attenuation level set at the attenuator [-54dBm, -62dBm]. This implies that the PRR drops from 100% to 0% over the range of RSS from [-81dBm, -89dBm]. We define this range as the *receiver's critical sensitivity band*. The 100% drop in PRR at values close to -89dBm can be explained by the fact that the minimum power required, by the mote's hardware, to decode the packets is

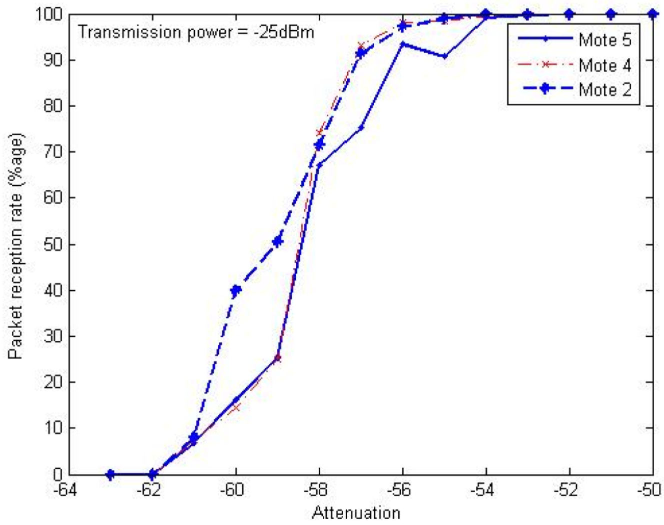

Figure 3.3: Receiver: PRR vs. RSS.

≈ -90dBm [2].

The result indicates that the PRR is largely dependent on the received signal power at the receiver, and asymmetric links can result if the RSS falls in the receiver's critical sensitivity band of ≈ [-80dBm, -90dBm]. Low transmission power, or excessive propagation losses as a result of long links, are responsible for the RSS in the critical sensitivity band. For a fixed transmission power WSN, link asymmetry can be reduced by selecting short links instead of long links by proper topology control.

3.4 Transmit-Receive Switching Mode

This section studies the switching effect of the motes, wherein a mote is simultaneously transmitting and receiving data packets. This is a very likely configuration in a group of wireless sensor nodes, wherein a couple of intermediate nodes may be simultaneously relaying packets, back and forth, between the sink and the source nodes. Another common scenario is that the BS may be receiving packets from different sources, and acknowledging them alongside its routine operations (such as data logging or transfer). We analyze this characteristic using MicaZ motes in experimental Setup-C & D.

Figure 3.4-(a) shows the difference in RSSI value, with the switching and non-switching mode at the BS (mote 0), for links 0→3, 0→5, and 0→7, for PL of 29 Bytes with different IPI. The RSSI values of the packets sent as acknowledgment by BS to the respective motes (from Setup-C) are compared with their corresponding values obtained from Setup-D (switching vs. non-switching). The result shows that the switching mode results in higher RSSI for links (0→3, 0→5), and lower RSSI for link (0→7). Note that link (0→7) is operating in the receiver's critical sensitivity band (RSS < -80dBm) (Section 3.3), which supports our observation that links operating in this power region can produce unexpected variations in RSS, and hence, lead to link asymmetry.

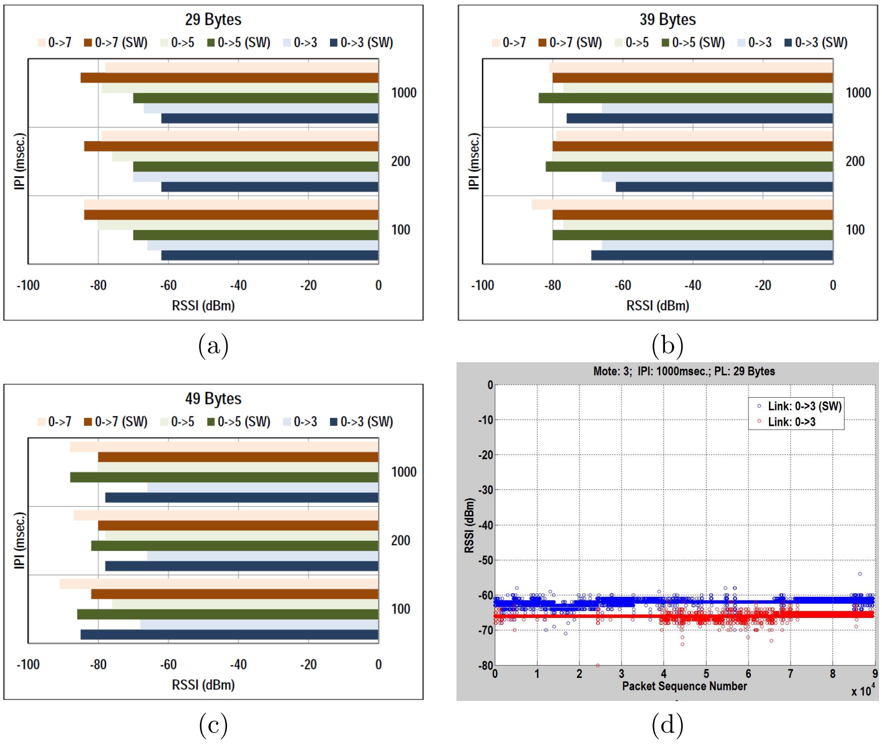

Figure 3.4: Switching effect on RSS.

All the cases show differences in RSS; its just that the trend is reversed for the link 0→7.

Figure 3.4-(b) shows the temporal statistics for the entire observation period, for the short link (of 1m) between BS and mote 3. The link 0→3 shows a higher RSSI value under switching effect, which is of the order of 2-4dBm. This experiment was repeated for different PL of 39 and 49 Bytes, and similar results have been reported in Figures 3.4-(b) and (c).

We conclude that there is a variation in power level, when a low-powered mote is operating under switching mode, and can be a cause of link asymmetry if this power difference goes high, and especially, if it is operating in the receiver's critical sensitivity band.

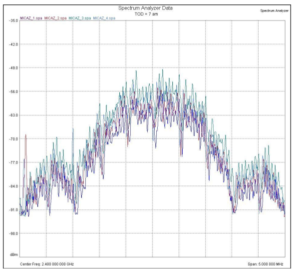

(a): 7am.

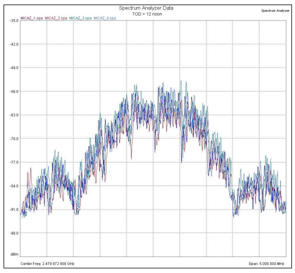

(b): 12noon.

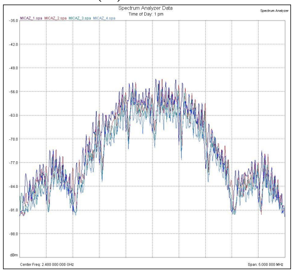

(c): 1pm.

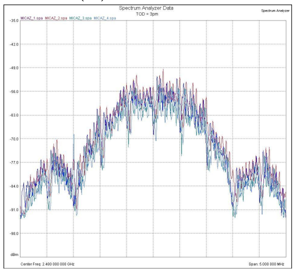

(d): 3pm.

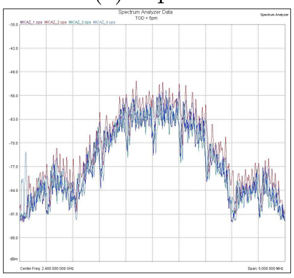

(e): 5pm.

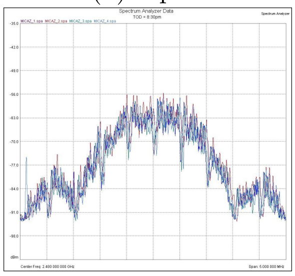

(f): 8:30pm.

Figure 3.5: Spectrum Envelope at different TOD.

3.5 Environmental Conditions

This section details the experimental findings on the effect of environmental factors on the link performance. It was performed using Setup-A, for a set of 4 different sender motes (MicaZ) at different time of the day over a period of one week. The environmental conditions for each set of time is described in Table 3.1.

Figure 3.5 shows the spectrum results for these experiments. The peak envelope (dBm) recorded by the 4 different motes (A,B,C,D) has been specified in Table 3.1. The spectrum results show that the spectrum envelope is not consistent during all the observations performed at different time of the day, and have a variance of $\approx$ 1-10dBm. One would expect this difference in RF power to effect WSN transmissions at different time of day under different environmental conditions. Under normal WSN operation, where both forward and reverse links are simultaneously operational, environmental conditions are expected to be similar, and hence, have negligible effect on link performance in both directions. However, if there is a substantial delay between these operations, wherein the environmental conditions change, then link asymmetry may become apparent.

Table 3.1: Environmental Conditions

Exp. No.	**Time of Day**	**Environmental Conditions**	**A**	**B**	**C**	**D**
1	7a.m.	21^{o}C, Wind: NW at 13 km/h, Humidity: 60%	-56	-56	-50	-53
2	12noon	19^{o}C, Wind: S at 27 km/h, Humidity: 56%	-60	-60	-53	-57
3	1p.m.	30^{o}C, Wind: SW at 8 km/h, Humidity: 29%	-53	-53	-56	-56
4	3p.m.	25^{o}C, Wind: NW at 21 km/h, Humidity: 28%	-53	-50	-53	-55
5	5p.m.	26^{o}C, Wind: N at 19 km/h, Humidity: 39%	-54	-52	-56	-56
6	8:30p.m.	21^{o}C, Wind: NW at 14 km/h, Humidity: 38%	-56	-53	-49	-51

3.6 Temporal Properties of Links

We describe links based on the PRR as suggested by Srinivasan et. al. in [7]. A link between a node pair is termed as poor, intermediate and good, if the PRR $< 10\%$, $10\% - 90\%$ and $> 90\%$ respectively. Cerpa et. al. in [8] has characterized good and bad links to remain invariant (or quite stable) in their autocorrelation of packet reception and losses, and intermediate links to have high correlation for successful packet reception than losses. Additionally, the number of intermediate links is always more than good or bad links. Therefore, we believe that intermediate links in low-power wireless devices are critical, as they carry the majority of data traffic, and can be engineered to attain their maximum potential level.

In this section, we analyze intermediate link properties of the wireless links, and characterize its dependence on IPI, PL and global differential link quality (GDLQ). The measurements have been taken using MicaZ motes in experimental Setup-C. Every transmitted packet consists of a fixed-length header consisting of the starting sequence of symbols and the default I-Frame (Interoperable Frame) CC2420 radio header, variable-length payload, and fixed-length footer consisting of the CRC. The acknowledgment packets have the same structure and length as the transmitted packets, wherein the values for the respective fields are only altered as per the requirement.

Inter-Packet Interval

We analyze the relationship between PRR and IPI in this section. Figures 3.6, 3.7 and 3.8 show the cumulative distribution function (CDF) of the PRR of every node pair (both forward and reverse links) in the configured topology. The y-axis of every plot has been labeled as $F(x)$, which indicates the (number of observations $\Leftarrow$ x)/(Total number of observations), where x represents the values in the x-axis. IPI is a representation for traffic load, as lower value of IPI result in increased traffic load, and vice versa.

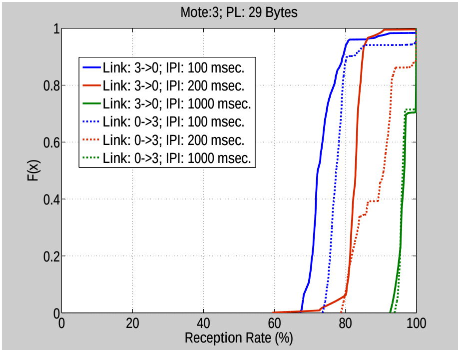

(a)

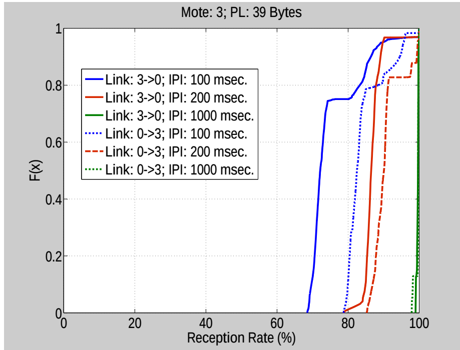

(b)

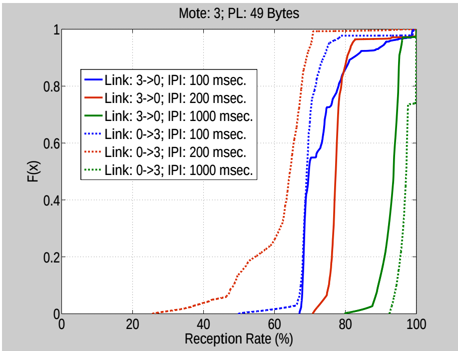

(c)

Figure 3.6: Mote 3: CDF of link qualities for different IPI and PL.

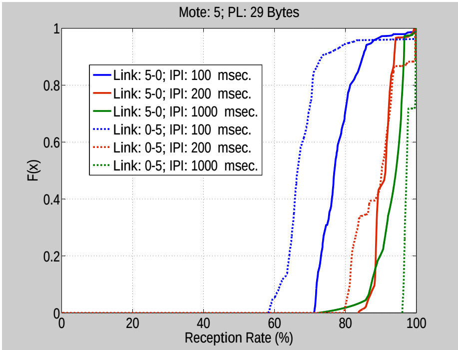

(d)

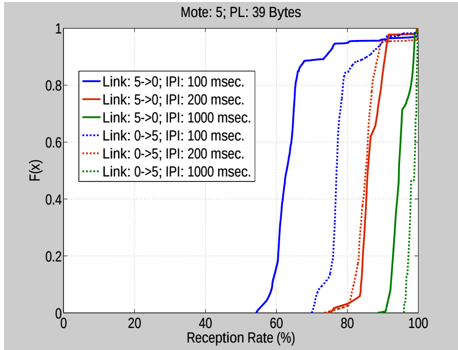

(e)

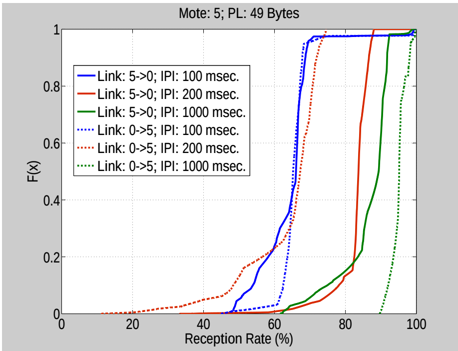

(f)

Figure 3.7: Mote 5: CDF of link qualities for different IPI and PL.

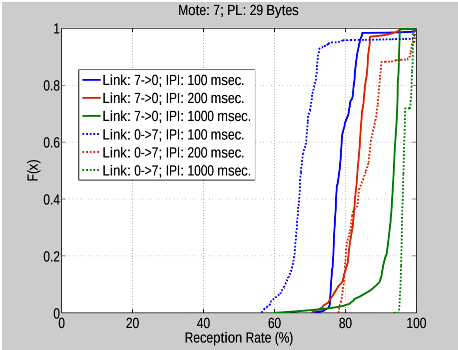

(g)

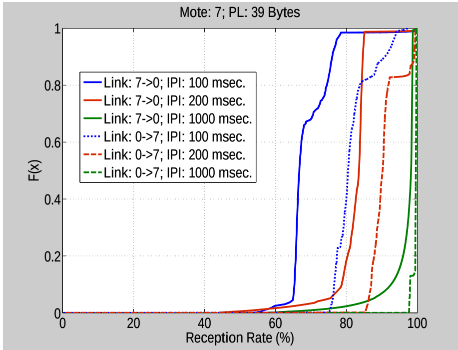

(h)

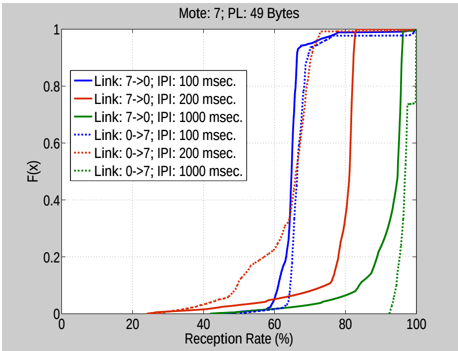

(i)

Figure 3.8: Mote 7: CDF of link qualities for different IPI and PL.

Figure 3.6-(a) shows that the minimum PRR achieved increases with the increase in IPI values for both forward and reverse links. The PRR values are 70%, 80% and 95% for link from mote 3 to BS, having IPI values of 100,200 and 1000 msec. respectively. Similar trends are observed for other links in the experiment. Comparing the minimum PRR obtained for different links, in Figure 3.6-(a), Figure 3.7-(d) & Figure 3.8-(g), we observe that the shorter links perform better as compared to the longer ones for different IPI values. Srinivasan et. al. in [7] have reported that the PRR of the reverse link (referred to as acknowledgment reception rate (ARR)) is more than the PRR of the forward link. Our results, also, show this link behavior, for intermediate links with higher IPI (i.e. less traffic load) and smaller PL (Figure 3.6-(a) & Figure 3.6-(b)). However, this relationship may not always hold for links with low IPI (i.e. high traffic load) with larger PL, as shown in Figure 3.7-(d), Figure 3.7-(f), Figure 3.8-(g) & Figure 3.8-(i).

These results, thus, highlight two important characteristics. First, the PRR increases with the decrease in the traffic load. For example, the minimum PRR improves by about 20-25% by increasing the IPI from 100 to 1000 msec. for different packet lengths. Second, the PRR of the forward and reverse links show large differences for high traffic load (low IPI), which diminishes with the increase in PL and IPI.

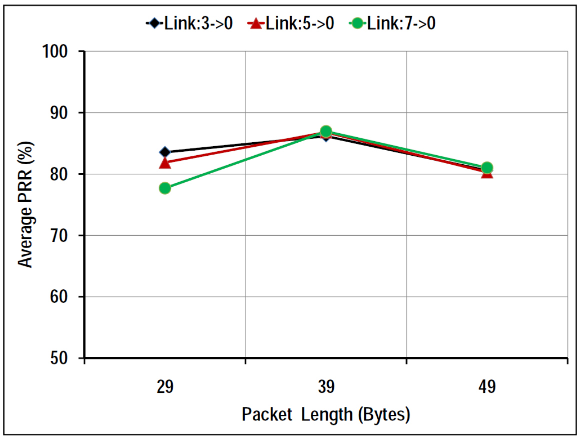

(a): Forward Link.

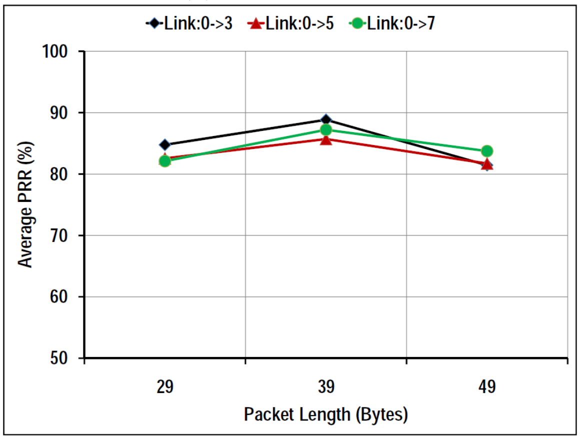

(b): Reverse Link.

Figure 3.9: PRR vs. PL.

Packet Length

In this section, we analyze how PL affects PRR. Figure 3.6, Figure 3.7, Figure 3.8 and Figure 3.9 shows the variation in PRR of the forward and reverse links as a function of PL.

By observing the sub-figures in Figure 3.6, 3.7 and 3.8, it is apparent that the best-case PRR (i.e. with low traffic load), for different link lengths, is not affected by the change in PL, where the PRR of the reverse link is always more than or equal to the PRR of the respective forward link. However, in the average and worst-case scenarios (with moderate to high traffic load), the performance of short links deteriorates with increase in PL (Figure 3.6-(c)). In addition, the PRR of the reverse path, for longer links shows better performance, in comparison to the forward path for the respective node set, with the increase in PL (Figures 3.7-(d)&(e) and Figures 3.8-(g)&(h)).

From Figure 3.9, we observe that the average PRR, initially, increases for the increase in PL from 29 Bytes to 39 Bytes, before decreasing again for further increase beyond 39 Bytes. This change is more profound for longer links (e.g. 7→0 and 0→7). This result fits well with the principle that smaller packets sent over long distances are more likely to get corrupted than longer packets, as they are less robust to multipath and interference effects of the communication medium.

The following two characteristics are highlighted from the results. First, it is beneficial to send small packets for short links. Second, PRR also depends on the PL, and there exists a threshold value for it, beyond which, the PRR starts decreasing.

Global Differential Link Quality

Global Differential Link Quality (GDLQ) of the system encapsulates the idea of identifying a specific period during the entire operational time that provides substantial asymmetry in the forward and reverse links. This metric looks at the system as a whole, and provides a quick snapshot of the system's link asymmetry characteristics.

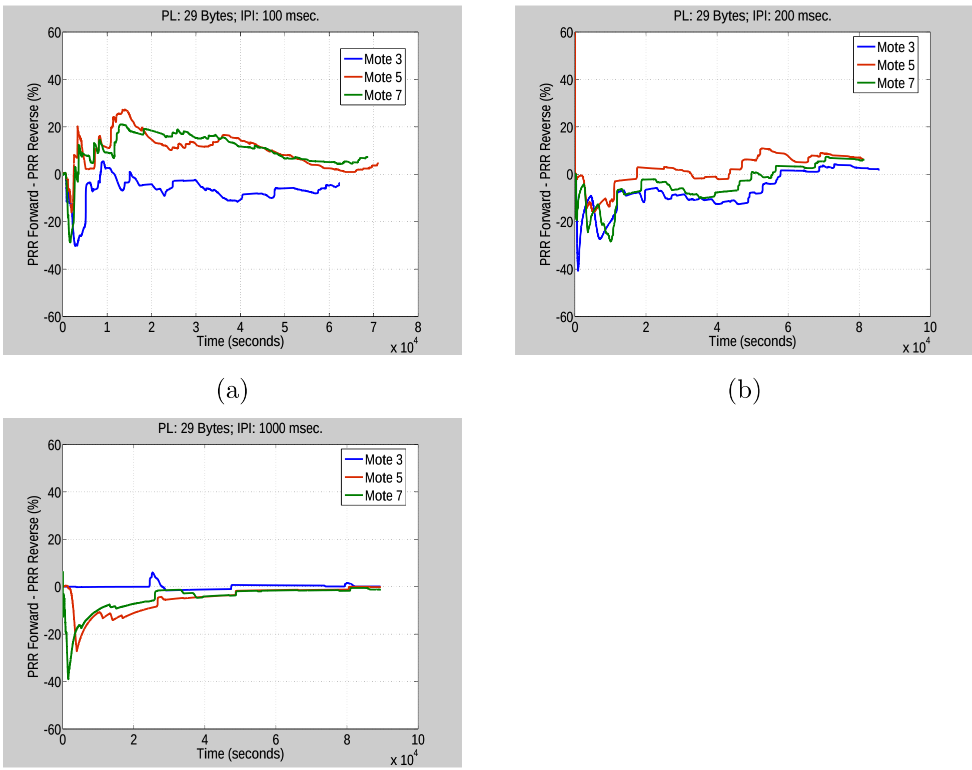

(a) (b) (c)

Figure 3.10: Global Differential Link Quality for different IPI and PL of 29 Bytes.

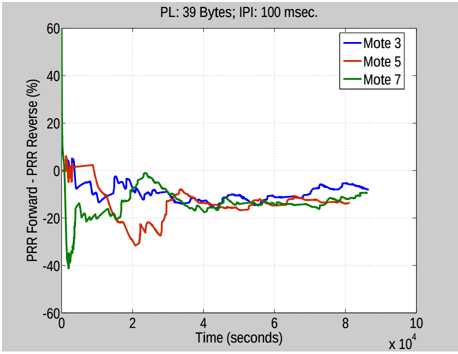

(d)

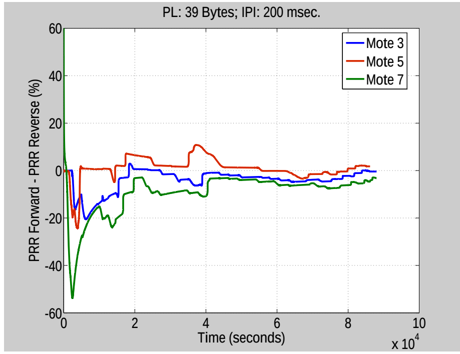

(e)

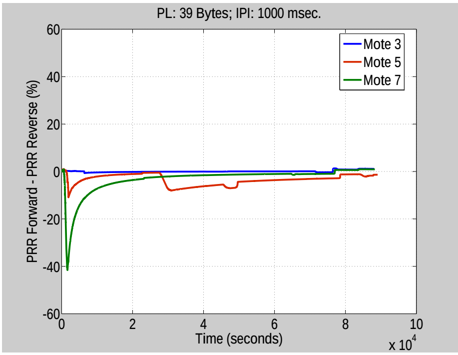

(f)

Figure 3.11: Global Differential Link Quality for different IPI and PL of 39 Bytes.

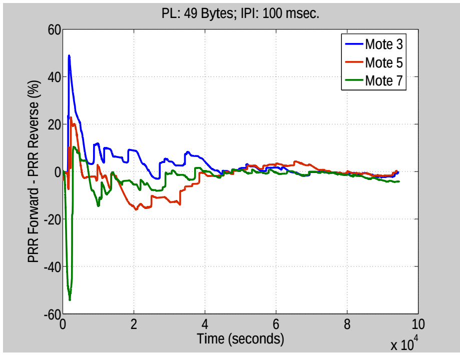

(g)

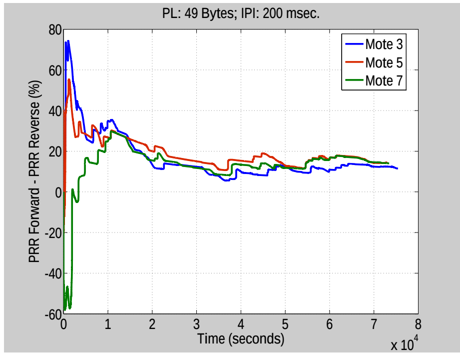

(h)

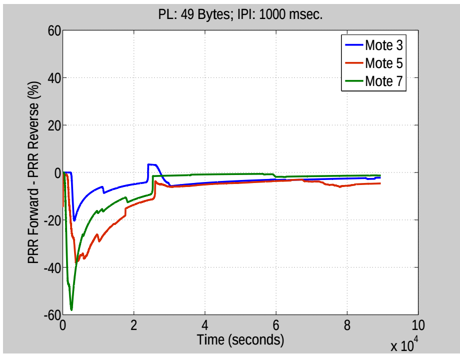

(i)

Figure 3.12: Global Differential Link Quality for different IPI and PL of 49 Bytes.

Figure 3.10, 3.11 and 3.12 shows the differential PRR (i.e. PRR of the forward link - PRR of the reverse link) as a function of time (seconds), for IPI of 100, 200 and 1000msec., and PL of 29, 39 and 49 Bytes. A value of 0% means that there is no asymmetry in the link behavior. From the results, we observe that all the links start with oscillations before settling down to a steady differential PRR value. This region of instability is predominantly during the first 8 hours of the experimentation period that coincides with regular office hours (11am-7pm), and hence, records the maximum packet drops in both the forward and reverse links. Observation data taken during this period show asymmetry nature of the links, however, this behavior diminishes during the remaining period of inactivity inside the experimentation environment. Neither the GDLQ, nor the global quality bandwidth [8] (Figures 3.13, 3.14 and 3.15) show any significant period of improved performance for the links during the period of office inactivity. Irrespective of the PL, links with low traffic load (high IPI) show nearly negligible link asymmetry (Figure 3.10-(c), 3.11-(f) & 3.12-(i)), while links with high traffic load (low IPI) show asymmetric behavior (Figures 3.10-(a) and (b), Figures 3.11-(d) and (e), 3.12-(g) and (h)).

The following two characteristics are highlighted from the results. First, observation data should be collected for a long time-period (with least external activity), to allow the differential PRR to decay with time. Second, low traffic load is preferable, as they have the least time-varying oscillations, and remain mostly constant around the 0% differential PRR level.

Discussion

From the observations reported in the previous sub-sections, it can be concluded that IPI has more impact on link asymmetry than PL. Therefore, a low-powered wireless link operating under high traffic load (low IPI) is more susceptible to asymmetry than a less loaded link with higher IPI. Instantaneous PRR may show unstable characteristics, but, such effects can be negated by operating the links for a long time duration.

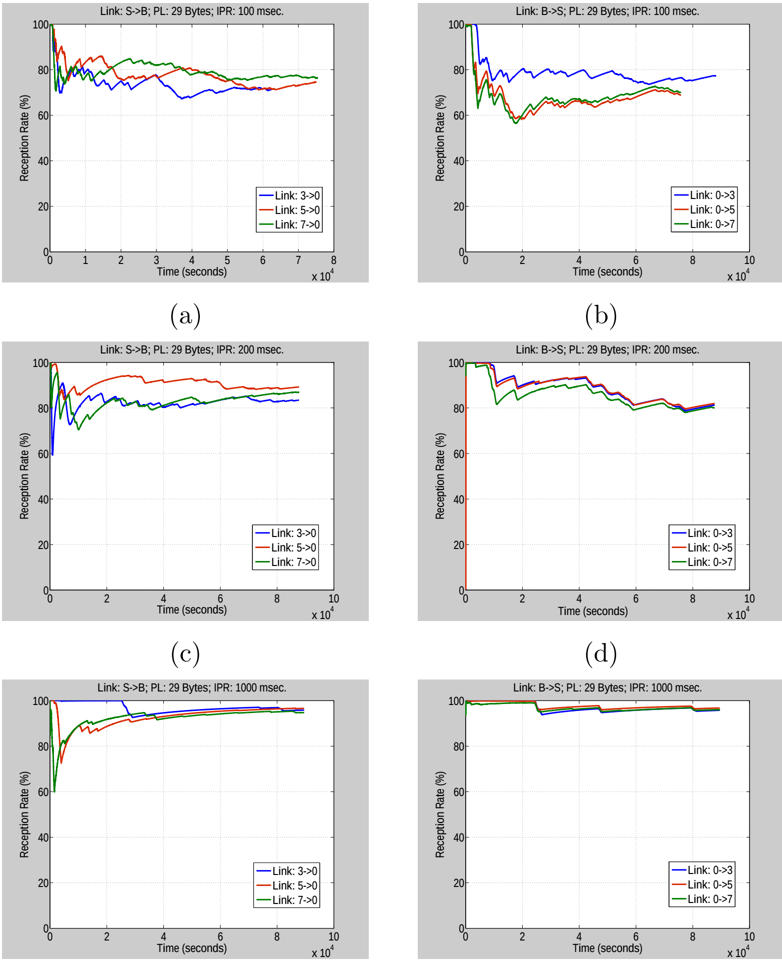

(a) (b)

(c) (d)

(e) (f)

Figure 3.13: PRR vs. Time for PL of 29 Bytes.

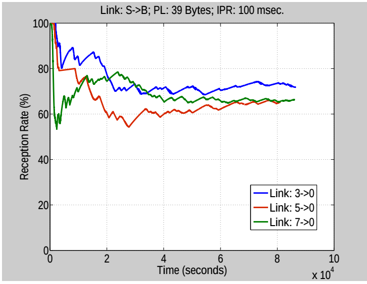

(a)

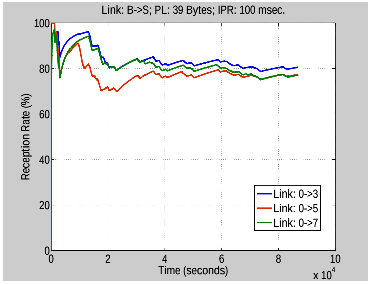

(b)

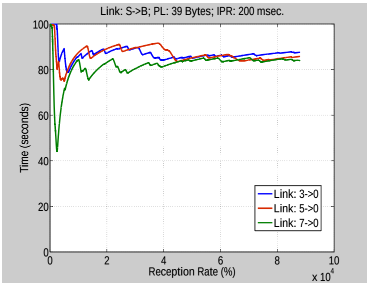

(c)

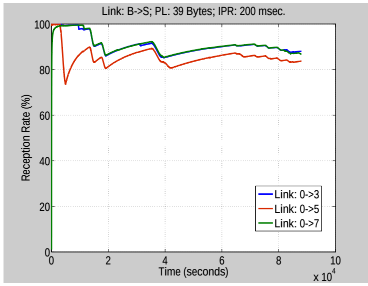

(d)

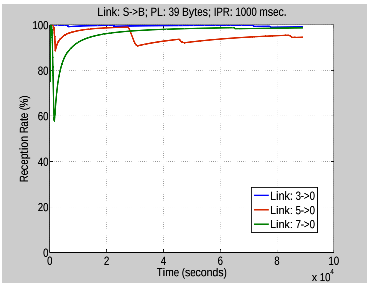

(e)

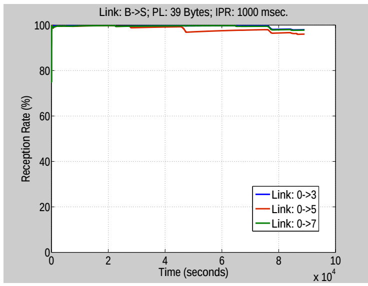

(f)

Figure 3.14: PRR vs. Time for PL of 39 Bytes.

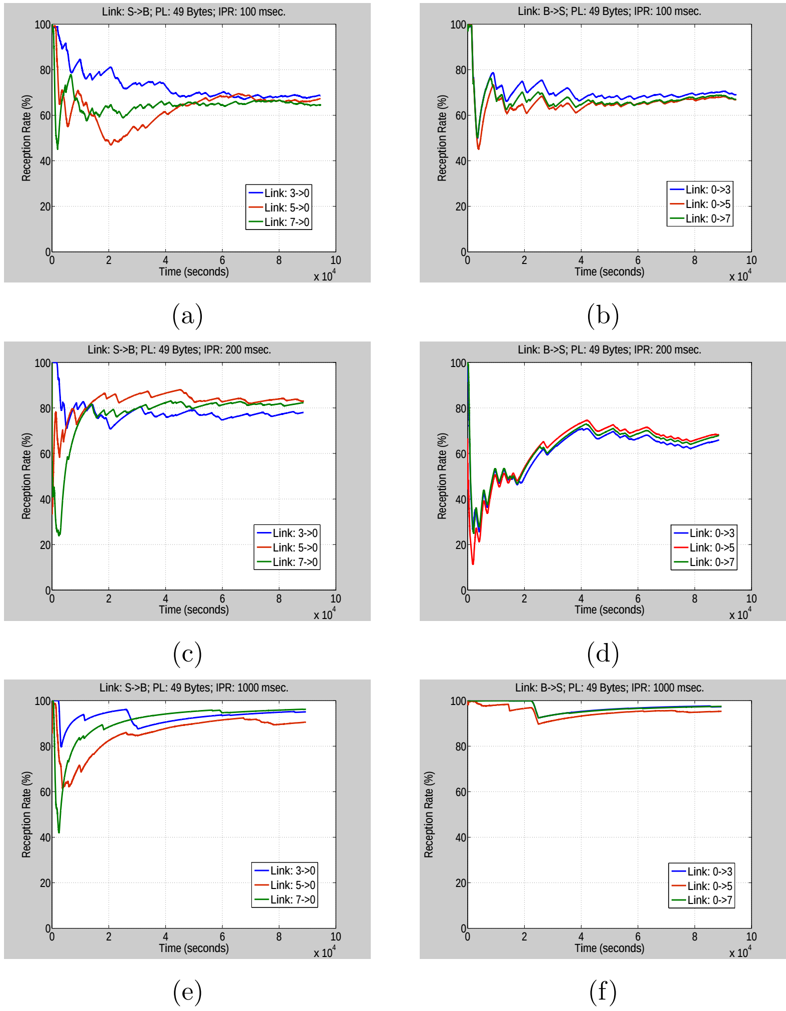

Figure 3.15: PRR vs. Time for PL of 49 Bytes.

4 Related Work

The problem of asymmetric links in low-powered sensor devices has been widely discussed in the vast array of existing literature. Liu et. al. in [6] have conducted field trials for the analysis of link asymmetry, and indicated that frequency misalignment between motes is a significant contributor to it, in addition to the motes transmission power. Ganesan et. al. in [9] have presented their studies for different layers in the protocol stack using Rene motes. They have suggested, through empirical data collection that the radio links (in low-powered devices) exhibit bi-directionality, provided statistics to measure the number of asymmetric links as a distance qualifier, and have attributed this behavior to differences in receiver's sensitivity and mote transmission power. This information has been further verified by Cerpa et. al. in [10]. Woo et al. in [11], through the packet loss models between the sending and receiving motes, demonstrated that the PRR is uncorrelated with large distances between node pairs, and hence concluded that differences in the mote's hardware (or radio) is the prime factor responsible for these asymmetries. Zhao et al. in [12] studied it with respect to different environments, power levels and coding schemes, and suggested multipath as one of the reasons for this behavior. As all of these previous studies had been conducted on older motes such as the Rene, Mica and Mica2, therefore, Zhou et. al. in [13] presented their finding on hardware mis-calibration, by experimenting with the ZigBee-compliant motes, as well as the older ones, and proposed a model to capture this characteristics. Cerpa et al. in [8] showed that the PRR is inaccurate to define long-term links as it does not account for the underlying loss distribution, and hence has utilized the required number of packets (RNP) as a measure to characterize the links. Srinivasan et. al. in [7] consider a link to be asymmetric if the difference in the forward and reverse PRR is more than 40%. They have suggested that asymmetric links are the outcome of the variation in per node RSSI and noise floor that affect the long term PRR.

5 Conclusion and Future Work

This paper characterizes the link asymmetry behavior in low-power wireless system, and may provide practical benefits to other researchers who are working on similar problems and projects. The experimental study presented in this paper has highlighted the following characteristics. Frequency misalignment is unlikely to be the cause of link asymmetry in WSNs as there is no major variation in the center frequency for different motes. The power variations due to antenna characteristics are also likely to have negligible affects. The major factors contributing towards it are difference in reception power of the motes within the receiver's critical sensitivity band of $\approx$ [-80dBm, -90dBm], switching mode of operation, environmental factors, and high traffic load. As future work, we plan to characterize links and their performance, with respect to different environmental conditions, and thus predict their behavior. We believe that an exhaustive study of the asymmetry of low-powered wireless links, and their characteristics would help to design more efficient protocols in the future.

Bibliography

[1] http://focus.ti.com/lit/ds/symlink/cc1000.pdf.

[2] http://focus.ti.com/lit/ds/symlink/cc2420.pdf.

[3] http://www.xbow.com/Products/Product_pdf_files/Wireless_pdf/MICA2_Datasheet.pdf.

[4] http://www.xbow.com/Products/Product_pdf_files/Wireless_pdf/MICAz_Datasheet.pdf.

[5] http://www.us.anritsu.com/products/MS2721A_Spectrum-Master_ARSPG_ARQQSidZ654.aspx.

[6] Ren P. Liu, Zvi Rosberg, Iain Collings, Carol Wilson, Alex Y. Dong, and Sanjay Jha. Overcoming radio link asymmetry in wireless sensor networks. In *International Symposium on Personal, Indoor and Mobile Radio Communications (PIMRC)*. IEEE, 2008.

[7] Kannan Srinivasan, Prabal Dutta, Arsalan Tavakoli, and Philip Levis. An empirical study of low-power wireless. *ACM Transactions on Sensor Networks*, 6(2):1–49, 2010.

[8] A. Cerpa, J. L. Wong, M. Potkonjak, and D. Estrin. Temporal properties of low power wireless links: modeling and implications on multi-hop routing. In *MobiHoc*, pages 414–425. ACM, 2005.

[9] D. Ganesan, B. Krishnamachari, A. Woo, D. Culler, D. Estrin, and S. Andwicker. Complex behavior at scale: An experimental study of low-power wireless sensor networks. Technical Report Tech. rep. CS TR 02-0013, 2002.

[10] A. Cerpa, N. Busek, and D Estrin. Scale: A tool for simple connectivity assessment in lossy environments. Technical Report Tech. rep. 0021.

[11] A. Woo, T. Tong, and D Culler. Taming the underlying challenges of reliable multihop routing in sensor networks. In *SenSys*, pages 14–27. ACM, 2003.

[12] J. Zhao and R Govindan. Understanding packet delivery performance in dense wireless sensor networks. In *SenSys*, pages 1–13. ACM, 2003.

[13] G. Zhou, T. He, S. Krishnamurthy, and J. A Stankovic. Models and solutions for radio irregularity in wireless sensor networks. *ACM Transactions on Sensor Networks*, 2(2):221–262, 2006.